American Industrial Hygiene Association Journal

ISSN: 0002-8894 (Print) (Online) Journal homepage: https://www.tandfonline.com/loi/aiha20

Experimental and Numerical Studies on the Impact of Work Practices Used to Control Exposures Occurring in Booth-Type Hoods

Michael R. Flynn , Bradley D. Lackey & Premkumar Muthedath

To cite this article: Michael R. Flynn , Bradley D. Lackey & Premkumar Muthedath (1996) Experimental and Numerical Studies on the Impact of Work Practices Used to Control Exposures Occurring in Booth-Type Hoods, American Industrial Hygiene Association Journal, 57:5, 469-475, DOI: 10.1080/15428119691014828

To link to this article: https://doi.org/10.1080/15428119691014828

Published online: 04 Jun 2010.

AMERICAN INDUSTRIAL HYGIENE ASSOCIATION JOURNAL 57:469–475 (1996)

Experimental and Numerical Studies on the Impact of Work Practices Used to Control Exposures Occurring in Booth-Type Hoods

AUTHORS
Michael R. Flynn[a]
Bradley D. Lackey[b]
Premkumar Muthedath[c]

[a]Department of Environmental Sciences and Engineering, University of North Carolina at Chapel Hill, CB# 7400, Rosenau Hall, Chapel Hill, NC 27599–7400; [b]Health and Hygiene, 5311 77 Center Dr., Suite 84, Charlotte NC 28217; [c]Exposure Control Technologies, 1807 Chevelle St., Raleigh, NC 27607

The observation that the between-worker variance component of exposure is significant for those performing the same tasks suggests that work practices are an important determinant of exposure. Decisions to implement engineering controls may be less than optimal if these work practices are not carefully identified. This study examines the position of the worker with respect to an object and the airflow direction in a large booth-type hood, and its implications for control of exposure. Experiments are conducted in a wind-tunnel using a mannequin and tracer gas techniques to measure exposures in the various positions at different air velocities. Smoke-wire, flow-visualization techniques are employed to correlate the exposures with the airflow patterns. Numerical predictions of these flow patterns and exposures compare favorably with experimental data, despite limitations. Further work is underway to examine more realistic situations such as spray-painting applications.

Keywords: airborne pollutants, between-worker variance, booth-type hood, computational fluid dynamics (CFD), exposure, work practices

Recent studies[1,2] call attention to wide variation in worker exposure even among those performing the same job. This between-worker component of variability, to some extent, can reflect how different people perform the same job, i.e., differences in their work practices. The implications of this observation for the control of occupational exposures to airborne pollutants is significant. It suggests that in some instances engineering controls may not be optimal, or that to be made so, training in work practices must be an integral part of the solution.

Effective control intervention depends on a clear understanding of the factors responsible for exposure, their interaction, the extent to which they can be modified, and the various associated costs. In essence, a model is needed to predict exposure for the tasks under consideration. Although there are different approaches to developing such a model, the method examined here relies on the use of computational fluid dynamics (CFD).

A worker's exposure to an airborne contaminant over a time period T is defined here as the usual time-weighted average, breathing-zone concentration:

$$C_{TWA} = \frac{1}{T}\int_0^T C_{BZ}dt \qquad (1)$$

Specification of breathing-zone concentration as a function of time is the goal of any model designed to predict exposure. The equations governing the distribution of a gas or vapor in air are the standard equations of fluid mechanics, i.e., conservation of mass, momentum, energy, and species. Aerosols are included with modifications to account for their peculiar properties, e.g., deviation from airflow and coagulation. With appropriate boundary and initial conditions, these equations define the general CFD model, with the potential, theoretically, to specify breathing-zone concentration as a function of time for any pollutant of hygienic significance.

The operative word in the preceding sentence is "potential." Despite the generality and the

This work was supported by NIOSH grant #5 R01 OH02858, "Computational Methods in Industrial Ventilation."

firm foundation in first principles, the use of CFD as a design tool in industrial hygiene applications is rare. This is due in part to the extraordinary variability and complexity of real world operations, as well as limitations in computer capabilities. As computational power increases, however, more simulations are likely to be employed, initially as analytic tools and eventually in actual designs. Part of this evolution must necessarily focus on what the important determinants of exposure are, and how to model them effectively.

A general theory of human exposure to airborne contaminants does not exist in a form helpful for most industrial applications. Mixing models, e.g., the dilution ventilation equations, are incapable of addressing spatial variability and local mixing phenomena. In addition, studies[3,4] indicate significant changes in concentration over relatively small distances in the vicinity of the body. A simple conceptual model of exposure to gas or vapor was developed for a hand-held source of passive tracer based on the concept of vortex-shedding.[5–7] This model was calibrated with a stationary mannequin oriented with back to the flow in wind tunnel studies. The resulting equation for the equilibrium breathing-zone concentration, expressed as a dimensionless fraction, is:

$$C_{BZ} \approx \frac{10G}{UHD} \qquad (2)$$

where G is the contaminant generation rate (in ft^3/min), U is the freestream air velocity (in ft/min) in the wind tunnel, H is the mannequin height, and D the width of the mannequin perpendicular to the freestream (both in ft). Although application of this model is limited, it points to the importance of generation rate and air velocity as well as worker size in determining exposure. Subsequent to the dimensional analysis and empirical studies used to develop Equation 2, numerical solutions of the Navier-Stokes equations, using discrete vortex methods, were employed to confirm the results and provide a basis for a more general model of exposure.[8–10]

One limitation of the models described above is the assumption of a stationary worker relative to the airflow. In reality, worker motion and changes in position are important. At least two previous papers[11,12] address the significance of a worker-orientation effect in actual field studies. In addition, obstacles are generally present, e.g., workpieces, machinery, and other people. To address these concerns a recent study[10] expanded the vortex methods described above to permit time-dependent calculations of air velocity fields around workers in the vicinity of objects in booth-type hoods.

This article combines the discrete vortex algorithm for velocity calculations with a "massless-particle trajectory" technique[9,13] to predict exposure and confirm the importance of the different work practices (positions). The term "massless-particle" refers to a computational particle and should not be construed as an aerosol. It is designed to model the transport of a gas or vapor. This technique provides a basis for developing exposure predictions.

Configuration A (see Figure 1) shows a worker in a typical position (airflow from behind the worker with source between worker and workpiece) in a booth hood. Configuration B shows the worker 90° to the direction of the airflow (sideways to the airflow, to the side of the object, and with source between worker and workpiece). This represents an alternate work practice for the same task within the booth. These two configurations are examined here both experimentally and numerically.

THEORY

Human exposure to airborne contaminants is governed by the laws of fluid mechanics, i.e., the concentration of a specific chemical agent in the breathing zone is determined by the generation rate of the species, and the air velocity field that transports it to the worker. The pertinent equations are the Navier-Stokes equations, a species transport equation, and the conservation of mass. These coupled, nonlinear, partial differential equations require appropriate boundary and initial conditions for their solution. In general, a numerical algorithm is required for all but the simplest of problems. The complexity of most industrial flows makes realistic simulation of exposure quite challenging even for relatively simple job tasks. At present, crude approximations are required.

An important phenomenon known as boundary layer separation occurs as air flows around objects, including the human body. The pertinent manifestation with regard to exposure is recirculation of the air on the downstream side of the body, i.e., the generation of wakes that may entrain contaminant. If the source of pollution is within such a wake, increased exposure may result. The nature of wakes and their interactions is complex, particularly for the time-dependent three-dimensional flows found in industrial applications. One simplification is to consider two-dimensional flow. This increases the ability to obtain numerical solutions to the governing equations for complex configurations, and also allows detailed studies of the accuracy of such solutions. The drawback, of course, is limited applicability to actual operations.

In this study two-dimensional, time-dependent calculations of the air velocity field around an ellipse and rectangle (worker and workpiece) in two different orientations relative to a uniform freestream are designed to simulate different work practices conducted in a large booth-type hood. The eventual desire was to examine spray-painting operations, although in the present study no attempt was made to include the spray gun or aerosol particles. Figures 2A and 2B show vector plots of the velocity field for the different configurations at a particular moment. As the velocity field evolves in time, a transport equation for the passive tracer contaminant is solved to obtain the concentration field. This is integrated over time to get exposure. Details of this procedure have been presented for the mannequin in uniform flow.[9] In this work the concentration algorithm is extended to the configurations shown in Figure 2.

An important issue in predicting exposure using numerical methods is to determine a region over which to average the concentration to obtain a reasonable breathing-zone estimate. This issue was examined previously[9] for a stationary mannequin oriented with back-to-flow and a hand-held source of tracer gas as contaminant. In that instance the recirculation zone downstream of the mannequin encompassed the source and provided a suitable averaging space, since it was in direct contact with the breathing zone. This is also the case for the configuration in Figure 2A; however, in Figure 2B the mixing zone is to the side of the worker and does not include the source. The implications are important with respect to obtaining accurate estimates of exposure.

METHODS

Numerical

Details of the specific numerical methods used in this work have been published[8–10,13] previously; only a brief summary is given

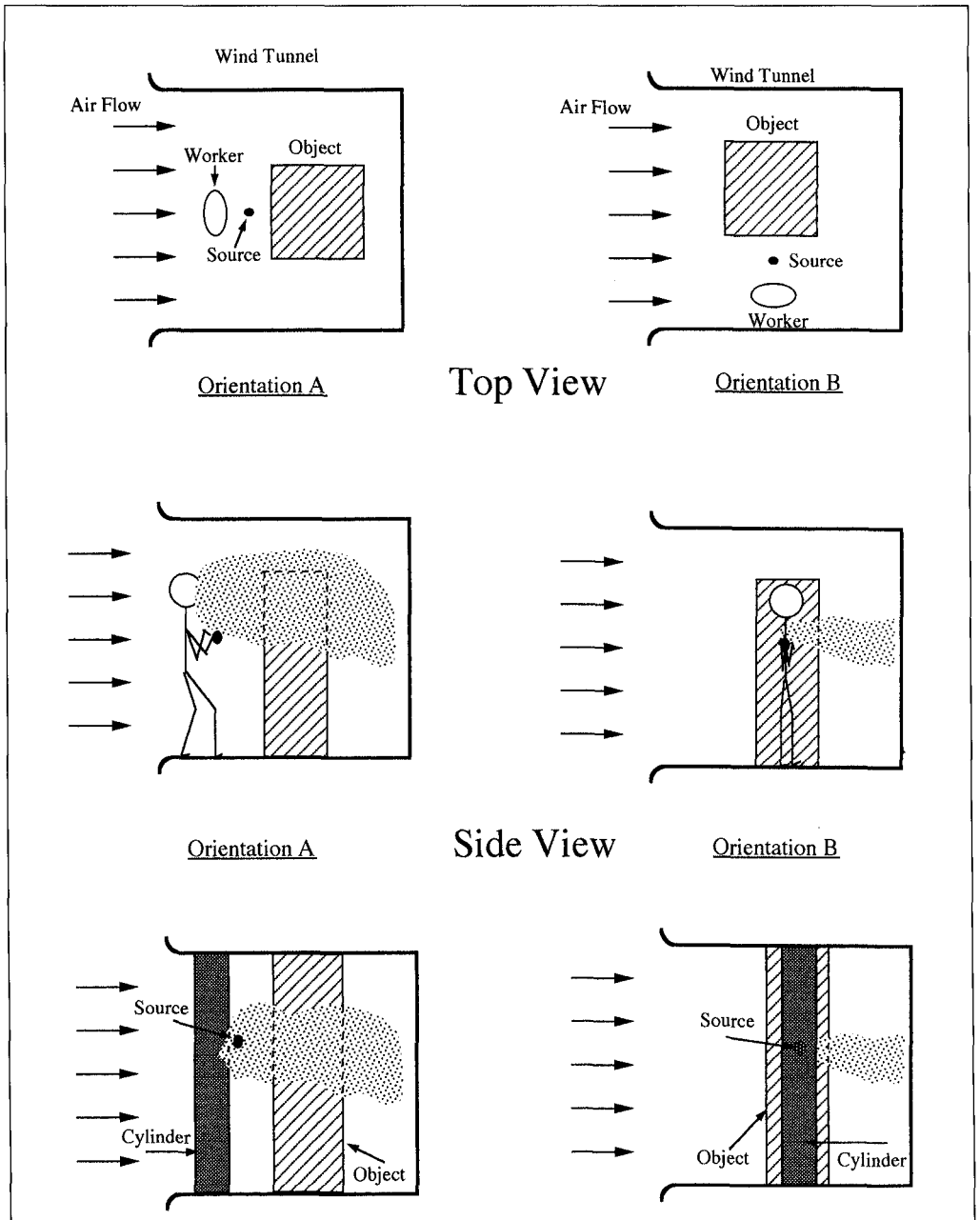

FIGURE 1. Experimental Configurations A and B, top and side views, in wind tunnel

here. The discrete vortex method is a technique for solving the time-dependent, incompressible Navier-Stokes equations in vorticity transport form. It relies on a decomposition of the velocity field into the sum of a potential and rotational component. At each time step, the method of fractional steps is used to split the vorticity transport equation into a Euler equation and a diffusion equation. The former is solved by a particle discretization of the vorticity field (vortex blobs). The velocity is recovered from the vorticity field and used to advance the vortex blobs. The diffusion equation is solved by a random-walk algorithm. The end result is a two-dimensional, time-dependent velocity field that can be displayed as a vector plot at any instant in time.

The velocity field is used to transport massless tracer particles to approximate a solution to the species transport equation and predict concentration fields. A technique developed by Turfus,[13] which permits some consideration of three-dimensional dispersion within the two-dimensional calculation, is employed here. The concentration field is temporally and spatially averaged. It is the determination of the computational breathing zone that is of concern in these calculations. Figures 3B and 3C illustrate two different spatial zones for time averaging the concentration field for Configuration B. In the case of Configuration A, the zone shown in Figure 3A is used, as there is little doubt as to its position; but in Configuration B there is little probability that contaminant near the source is available for inhalation due to the essentially potential flow in that zone. It seems more likely that contaminant entrained into the downstream wake, as shown in Figure 3B, would be available for inhalation, as this wake is connected to the breathing zone. This issue is examined further in the Results section.

The numerical calculations are conducted using a 2 ft (0.61m) square to represent the workpiece, an ellipse 2 ft (0.61m) wide by 1 ft (0.30m) deep to represent the worker, and velocities to obtain the same Reynolds numbers as the experimental conditions. Concentrations are calculated in a dimensionless form for appropriate scaling to experiments. This procedure ensures dynamic and geometric similarity and economizes on computational effort. The dimensions for the numerical breathing zones shown in Figures 3A and 3C are 2.5 ft wide by 3.0 ft long; while for Figure 3B the dimensions are 1.5 ft wide by 3.5 ft long.

Experimental

Experimental studies were carried out in a low-speed, open-circuit wind tunnel 1.52 m square and 2.44 m deep (5 ft × 5 ft × 8 ft), with a velocity range of 0.127–1.40 m/sec (25–275 ft/min). The tunnel entrance was equipped with a flared flange, and the rear wall consisted of pegboard with .064 cm (0.24 inches) diameter holes to provide uniform air distribution across the tunnel. Observation windows on one side and the top of the wind tunnel were used for the flow visualization photos. A commercial mannequin, 1.04 m (41 inches) tall and 20 cm (8 inches) wide at the chest, was placed at the centerline of the tunnel. A wooden box, 0.41 m (16 inches) square and 1.12 m (44 inches) tall was placed roughly arm's length away (25 cm; 10 inches) to represent the workpiece.

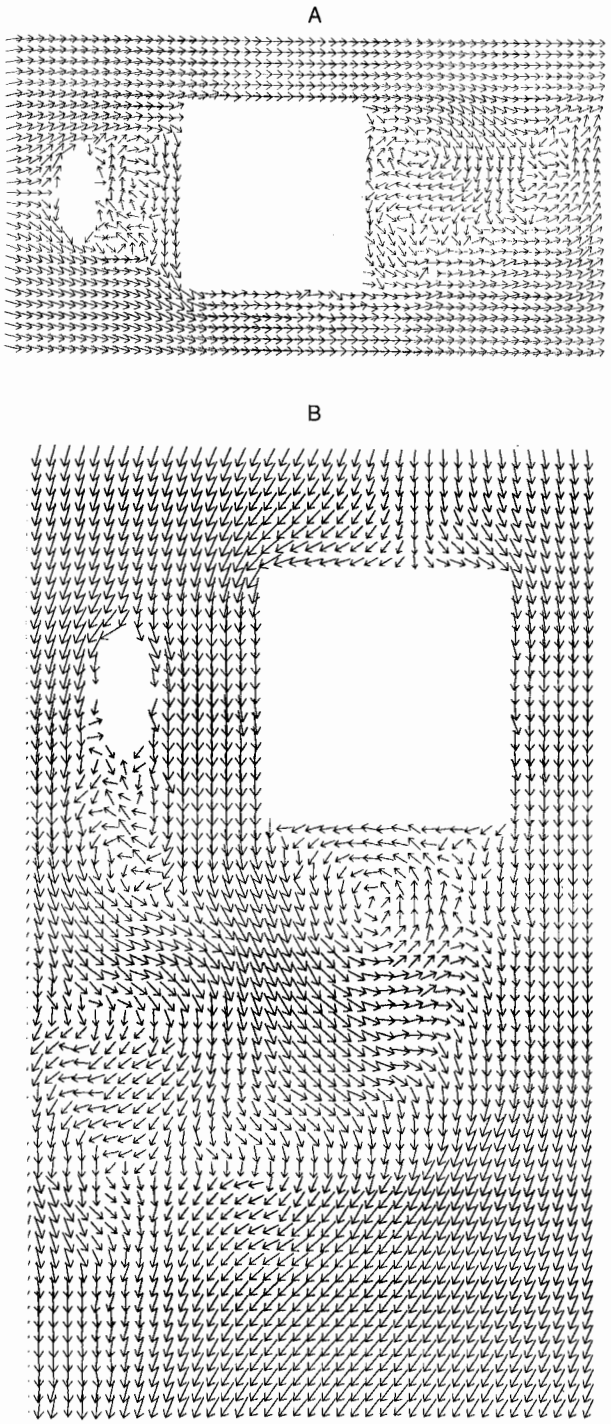

FIGURE 2. (A) Vector plot of numerically predicted instantaneous velocity field for Configuration A; (B) Vector plot of numerically predicted instantaneous velocity field for Configuration B

A neutrally buoyant mixture of 10.0% sulfur hexafluoride, 45.8% helium, and 44.2% air was used as a tracer. The mixture was released through a .25-inch diameter ceramic sphere at 220–230 cc/min (0.0008 ft^3/min of pure SF_6, 0.0036 ft^3/min of air, and 0.0037 ft^3/min helium). Pores in the sphere allowed the gas to diffuse in all directions. The source of contaminant was placed between the mannequin and the box at chest level in the mannequin's hands at a height of 79 cm (31 inches) and a distance from the box of 15 cm (6 inches) to simulate a typical work orientation.

An electron capture detector (ECD) was used to measure the concentration of SF_6 tracer gas. A sampling tube was connected from the mannequin's mouth, through the back of the head, to the sampling port of the detector nozzle. Air was continuously drawn through the mannequin's mouth at a flow of approximately 100 cc/min. Experiments were carried out in freestream velocities of 100, 150, and 250 ft/min. Reynolds numbers associated with these velocities are 6837, 10256, and 17092, respectively, based on a mannequin width of 20 cm (8 inches). The system was allowed to equilibrate for approximately 5 min before data were gathered. Two blocks, i.e., repetitions on separate days, of three to six trials were conducted for each configuration at each of the three airflows. Each block consisted of 300–600 data points collected by noting the ECD display at 5 sec intervals.

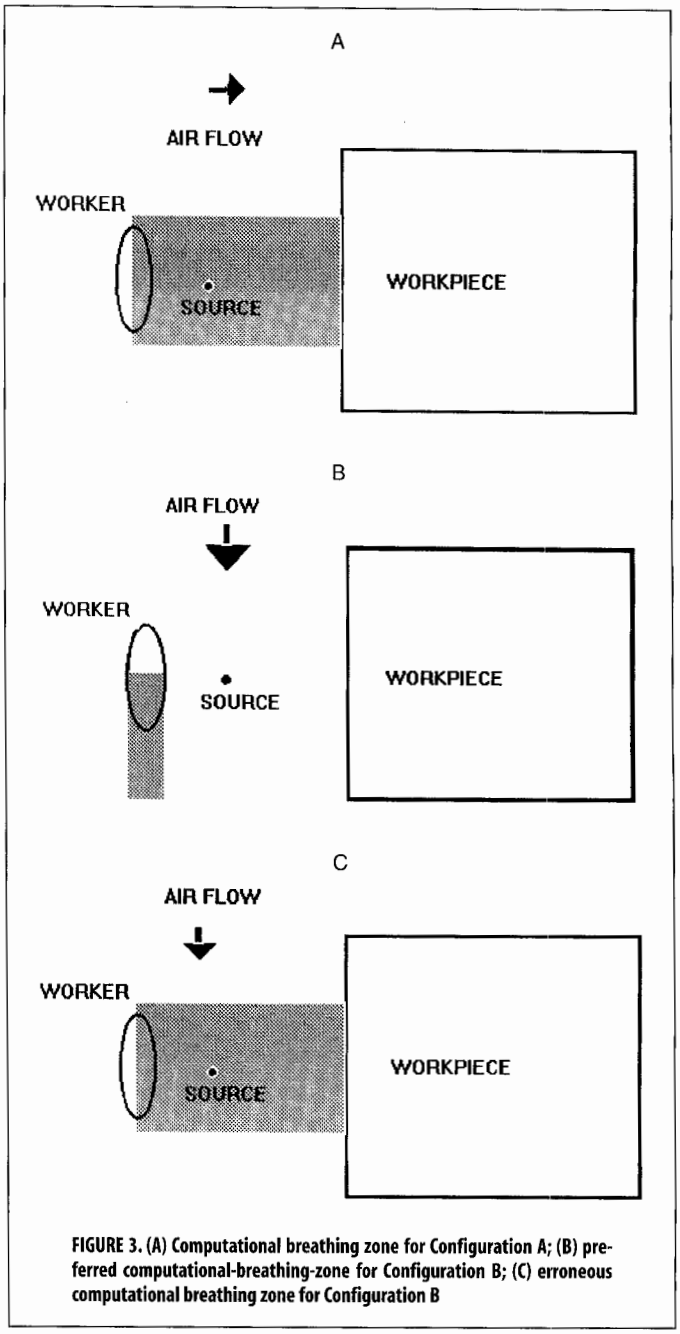

FIGURE 3. (A) Computational breathing zone for Configuration A; (B) preferred computational-breathing-zone for Configuration B; (C) erroneous computational breathing zone for Configuration B

Smoke generation techniques introduced[14] and refined[6] in previous work were used to visualize airflow around the mannequin and object. Several strands of 0.01-inch diameter nichrome wire were twisted together, coated with paraffin oil, and strung across the sampling region. A variable DC power source was connected to each end of the wire to provide current and heat the smoke-generating oil. A dense white smoke was produced for periods of 20–40 sec in the plane of the airflow. Photographs were obtained through the windows in the side and top of the wind tunnel.

Results and Discussion

Experimental

Concentrations measured in the breathing zone of the mannequin resulted in 12 mean values; one for each combination of configuration, airflow, and block. Table I shows the summary data in the format used for statistical analysis. The overall mean concentration was calculated by taking the mean of Block 1 times the number of data points in Block 1 plus the mean of Block 2 times the number of data points in Block 2 all divided by the total number of data points. The overall mean is the observed value used to compare with the values determined by numerical simulation.

Configuration A (airflow from the back) shows dramatically higher breathing-zone concentrations than Configuration B (airflow from the side). Table I shows that orienting the mannequin sideways to the airstream (as opposed to airflow from the back) results in a reduction of breathing-zone concentration of 187-fold at 100 ft/min freestream velocity, 994-fold at 150 ft/min, and 137-fold at 250 ft/min. Figure 4 illustrates the breathing-zone concentrations for Configurations A and B at the different air velocities.

Table II gives the results of two-way Model I analysis of variance (ANOVA) conducted using the data in Table I. Sulfur hexafluoride concentration is the dependent variable, with air velocity and position as fixed effects. The interaction term between velocity and position is significant at the $p=0.002$ level. This interaction indicates that while higher airflows result in reduced breathing-zone concentrations for Configuration A, the same trend was not noted in Configuration B. In fact, an initial decrease in exposure with velocity is noted up to 150 ft/min, and then an increase as velocity approaches 250 ft/min. This may reflect enhanced contaminant transport due to small-scale turbulence in the freestream or, more probably, limitations of the experimental methods. The overwhelming significance of the position effect ($p<0.0005$) is clearly evident even without the ANOVA.

The flow visualizations in the photographs (Figures 5–7) clearly show the airflow patterns around the mannequin in each configuration. Figure 5 uses a vertical smoke-wire 6 inches downstream of the mannequin to produce smoke from the plane of the contaminant release point. The smoke from eye-level down is drawn back toward the mannequin. From eye to chin level the backwash effect is less pronounced, but below chin level, almost all of the smoke is drawn back to the mannequin's body. The distinct separation of the airflow into an upper region rotating clockwise and a lower region rotating counter-clockwise was not evident as in an earlier study.[7] The area from the top of the head to the nose may be affected by the downwash effect over the top of the mannequin's head. Figure 6 shows a top view for Configuration A at a freestream velocity of 150 ft/min.

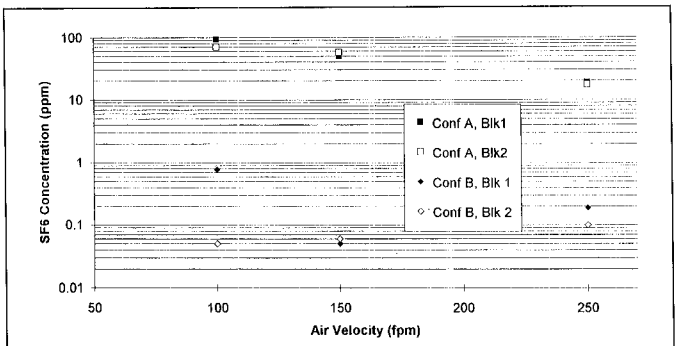

FIGURE 4. Experimental concentrations for Configurations A and B, Blocks 1 and 2, as a function of wind tunnel velocity

Figure 7 shows the mannequin in Configuration B at a flow of 150 ft/min. The streamlines are distinct around the mannequin and box, and without the visible mixing shown in Figure 6. Not visible in the photograph are the eddies downstream of the mannequin and box. Also, the streamlines past the contaminant source do not seem to be disturbed, and flow from the hand region to the breathing zone is not evident.

The roughly two to three orders of magnitude difference in concentration between the two configurations is attributed to reverse flow regions. As illustrated in Figures 5 and 6 , the reverse flow region for Configuration A includes the source. This draws contaminant back toward the mannequin. For Configuration B, the reverse flow region still forms, but it is downstream of the worker and workpiece and does not encompass the contaminant release point.

Numerical

Figures 2A and 2B illustrate typical vector plots of the instantaneous velocity fields for the two different configurations. Configuration B concentrations were averaged for two different computational breathing zones, as shown in Figures 3B and 3C, and one zone for Configuration A, Figure 3A. These zones are indicated by shading in the figures and are approximate only. The concentrations were averaged for a 1-min period during an interval where the mean value was stationary. In other words, the concentration was allowed to reach equilibrium before a spatial and temporal average was calculated.

TABLE I. Experimental Concentrations (ppm)

	Configuration A			Configuration B		
Air Velocity (ft/min)	100	150	250	100	150	250
Block 1	93.0	50.0	19.0	0.78	0.05	0.19
Block 2	70.0	57.6	17.5	0.10	0.06	0.10
Mean	83.2	53.7	18.2	0.44	0.05	0.13

TABLE II. Two-Way Analysis of Variance

Dependent Variable CONC			N = 12	Multiple R: 0.988	
Source	sum-of-squares	df	mean-square	F-ratio	P
Velocity	2028.143	2	10144.071	20.643	0.002
Position	7794.225	1	77944.225	157.667	<0.0005
Velocity Position	1993.124	2	996.562	20.287	0.002
Error	294.74	6	49.123		

FIGURE 5. Flow visualization for Configuration A side view at 150 ft/min. Smoke wire is between the mannequin and box.

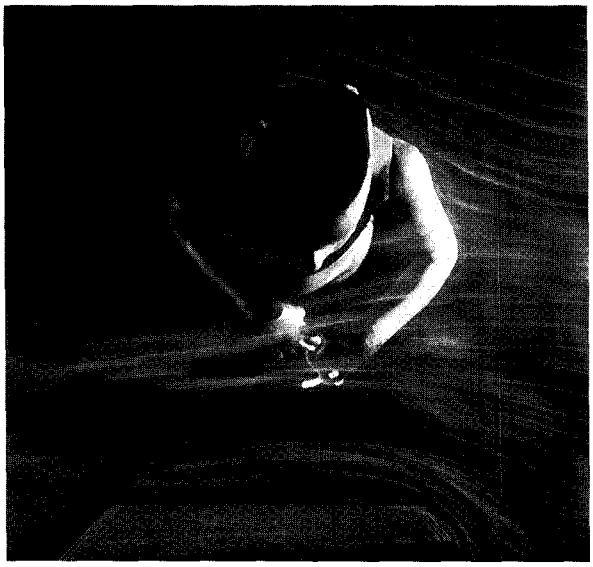

FIGURE 7. Flow visualization for Configuration B top view at 150 ft/min. Smoke wire is upstream of mannequin and box.

Table III presents the results of the numerical and experimental studies for a freestream velocity of 150 ft/min. The flow of SF_6 in the computer simulation is set to match the experimental value of 0.0008 ft^3/min of pure tracer. As shown in the table, the agreement between prediction and measurement for Configuration A is very good. The agreement for Configuration B clearly depends on selecting the near-wake region as the computational breathing zone. This makes sense if one considers that there is very little probability of contaminant near the source reaching the mannequin in Configuration B due to the essentially potential flow in that region. It is only when contaminant is entrained into the wake that mixing back to the mannequin is possible.

The qualitative agreement between the computed velocity fields and the experimental flow visualization is good. The computer simulation (Figure 2B) correctly identifies the essentially potential-laminar flow in Configuration B (photo in Figure 7) responsible for the reduced exposure. In addition, the strong mixing zone created by Configuration A is also captured in the simulation (Figure 2A) and confirmed by flow visualization (Figures 5 and 6). Numerical visualization of flow for possible control interventions is a potential design tool, much as the smoke tube is an evaluation tool in field studies.

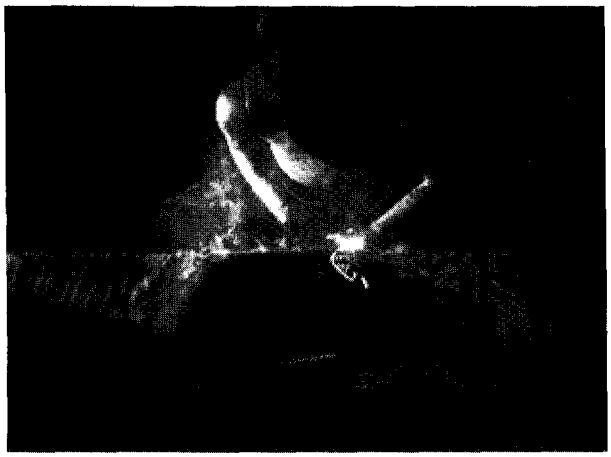

FIGURE 6. Flow visualization for Configuration A top view at 150 ft/min. Smoke wire is between the mannequin and box.

CONCLUSIONS

Experimental results, including flow visualizations, show that worker position relative to airflow can play a significant role in exposures generated by a hand-held contaminant source of negligible

TABLE III. Comparison of Concentrations (ppm) at 150 ft/min Air Velocity

	Computed Value	Measured Mean
Configuration A computational breathing zone as shown in Fig. 3A	41.8	53.7
Configuration B computational breathing zone as shown in Fig. 3B	0.4	0.05
Configuration B computational breathing zone as shown in Fig. 3C	29.0	0.05

momentum. Data show 2–3 orders of magnitude difference in concentration between the two positions. This difference is attributed to the formation of reverse flow regions immediately downstream of the worker and its relationship to the source and breathing zone. When an object is present, e.g., a workpiece, it may interfere with contaminant removal mechanisms such as vortex formation and shedding. Distinct reverse flow eddies, visible when just the worker and source are present in the freestream, do not form as readily when an object is placed downstream. The disturbance caused by an object is less pronounced when the airflow is from the side.

Two-dimensional numerical simulations of the velocity field obtained using vortex methods provide good qualitative agreement with flow visualizations obtained using smoke-wire techniques. A particle trajectory algorithm was used with these velocity fields to estimate tracer gas exposures to mannequins in wind tunnel studies. Predictions are in reasonable agreement with measured values and correctly identify the superiority of work position B over A. The potential exists to use computational fluid dynamics both as a qualitative and quantitative tool to estimate the impact of alternate work practices and their interaction with ventilation.

These simulations and experiments represent idealized conditions for the configurations studied. In a real booth operation many of the factors held constant in the experiment will vary. Worker motion and source momentum are perhaps the most significant limitations of this work. As a worker moves, new reverse flow regions are constantly forming and shedding. This may create eddies that draw contaminant into the worker's breathing zone even while the worker is standing perpendicular to airflow. In a compressed-air spray paint operation, the paint is delivered under pressure. The droplets will not follow the airflow, and the overspray may dramatically alter the flows predicted here.

A particularly important aspect of using two-dimensional simulations is confirmation of conclusions with experimental study. The booth-type arrangement employed here had a sufficiently two-dimensional flow pattern so that the simulations were reasonable as shown with flow visualization. The use of such an approach with a flow that is dominated by three-dimensional effects may not be as successful. Further study is recommended to examine the effects of object size/shape and source momentum on the breathing-zone concentrations. More realistic three-dimensional simulations are needed, as well as some way to incorporate the variability of boundary conditions into the numerical approach.

REFERENCES

1. **Kromhout, H.E., E. Symanski, and S.M. Rappaport:** A comprehensive evaluation of within- and between-worker components of occupational exposure to chemical agents. *Ann. Occup. Hyg. 37*:253–270 (1993).
2. **Rappaport, S.M., H.E. Kromhout, and E. Symanski:** Variation of exposure between workers in homogeneous exposure groups. *Am. Ind. Hyg. Assoc. J. 54*:654–662 (1993).
3. **Rodes, C.E., R.M. Kamens, and R.W. Wiener:** The significance and characteristics of the personal activity cloud on exposure assessment measurements for indoor contaminants. *Indoor Air 2*:123–145 (1991).
4. **Pengelly, M.I., J.A. Groves, R.D. Foster, P.A. Ellwood, et al:** Development of a method for measuring exposure to resin acids in solder fume. *Ann. Occup. Hyg. 38(5)*:765–776 (1994).
5. **George, D.K., M.R. Flynn, and R. Goodman:** The impact of boundary layer separation on local exhaust design and worker exposure. *Appl. Occup. Environ. Hyg. 5*:501–509 (1990).
6. **Kim, T.H. and M.R Flynn:** Airflow pattern around a worker in a uniform freestream. *Am. Ind. Hyg. Assoc. J. 52*:287–296 (1991).
7. **Kim, T.H. and M.R. Flynn:** Modeling a worker's exposure from a handheld source in a uniform freestream. *Am. Ind. Hyg. Assoc. J. 52*:458–463 (1991).
8. **Flynn, M.R. and C.T. Miller:** Discrete vortex methods for the simulation of boundary layer separation effects on worker exposure. *Ann. Occup. Hyg. 35(1)*:35–50 (1991).
9. **Flynn, M.R., M. Chen, T. Kim, and P. Muthedath:** Computational simulation of worker exposure using a particle trajectory method. *Ann. Occup. Hyg. 39(3)*:277–289 (1995).
10. **Kim,T. and M.R. Flynn:** Numerical simulation of airflow around multiple objects using the discrete vortex method. *J. Wind Engnr. Ind. Aerodynamics. 56*:219–234 (1995).
11. **Heriot, N.R. and J. Wilkinson:** Laminar flow booth for the control of dust. *Filtr. Sep.* March–April, pp. 159–174 (1979).
12. **Piney, M., F. Gill, C. Gray, D. Jones, et al.:** Air contaminant control: the case history approach—learning from the past and looking to the future. In *Ventilation '88 Proceedings of the Second International Symposium on Ventilation for Contaminant Control.* J.H. Vincent, ed. U.K.: Pergamon Press, 1989.
13. **Turfus, C.:** Calculating mean concentrations for steady sources in recirculating wakes by a particle trajectory method. *Atmos. Environ. 22(7)*:1271–1290 (1988).
14. **Tsanis, I.K.:** "Flow visualization in circulation air flows using the smoke-wire technique." Paper presented at the Fourth International Symposium on Flow Visualization, Paris, France, August 1986.